Supporting Information for: Investigation of the Impact of Lipid Acyl Chain Saturation on Fusion Peptide Interactions with Lipid Bilayers

William T. Heller[a], Piotr A. Zolnierczuk[a]

[a]*Neutron Scattering Division Oak Ridge National Laboratory, Oak Ridge, TN 37831, USA*

Preprint submitted to BBA Biomembranes *February 10, 2023*

1. Purity Assessment of the gp41rk Peptide

HPLC REPORT

Order Number	:SP200159
Name	:peptide_1 (21)
Sequence	:RKGIGALFLGFLGAAGSTMKR-Amidation
Lot. No	:GT90771/SP200159
Pump A	:0.1%Trifluoroacetic in 100% water
Pump B	:0.1%Trifluoroacetic in 100% acetonitrile
Total Flow	:1ml/min
Wavelength	:214nm
Analytial column type	:SHIMADZU Inertsil ODS-SP(4.6*250mm*5um)
Dissolution method	:100%H2O
Inj. Volume	: 25ul

Time	Module	Action	Value
0.01	Pumps	B.Conc	20
25.00	Pumps	B.Conc	85
30.00	Pumps	B.Conc	100
38.00	Pumps	B.Conc	100
40.00	Pumps	B.Conc	20
50.00	Controller	Stop	

Chromatogram

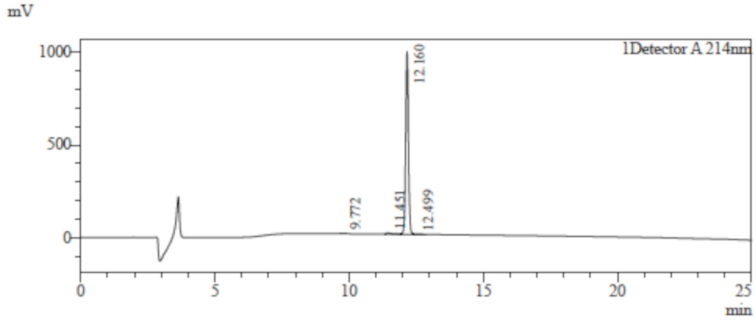

Peak Table

Detector A 214nm

Peak#	Ret. Time	Area	Height	Area%
1	9.772	8765	1670	0.12
2	11.451	82407	7852	1.14
3	12.160	7127113	986392	98.23
4	12.499	37139	2293	0.51
Total		7255424	998208	100.00

Figure S1: HPLC of the gp41rk peptide used for this study that was provided by Biomatik USA, LLC (Wilmington, DE) in the certificate of analysis.

2. Model for SANS Data Analysis

The SANS data were analyzed using a 3-shell vesicle model, similar to previous work [1, 2, 3]. The radius of the vesicle core was fixed to 500 Åduring data fitting, as was done previously [1, 2, 3]. While it was not possible to fix the polydispersity to 0.3, as was done in the previous work [1, 2, 3], because *sas_temper* cannot do so, it was constrained to be between 0.30000

and 0.30001. The structural model of the lipid bilayer for the three shells is based on the volumetric description of a lipid bilayer that was provided by Nagle and Tristram-Nagle [4]. Specifically the model follows the version of the volumetric model presented in the right panel of Figure 2C [4]. The schematic of the bialyer model is shown in Figure S2. Consider a lipid bilayer described by its steric thickness, D_b, which is related to the hydrocarbon chain thickness, D_{hc}, and the thickness of the headgroup, D_{hg}. Then, D_b is related to D_{hc} and D_{hg} through

$$D_b = 2D_{hc} + 2D_{hg}. \tag{1}$$

The value of D_{hc} is related to the area per lipid, A_L, and the lipid chain volume, V_c through the relation

$$D_{hc} = V_c/A_L. \tag{2}$$

The value of A_L that is used here for the mixed lipid bilayers studied is the average area per lipid, and it is one of the free parameters used in the SANS data analysis. The volume of the lipid chains, V_c, is calculated using the values presented in Table 1 and the composition of the sample being modeled. The value of D_{hg} used in the modeling was the value for PC bilayers (9 Å) that was presented in Reference [4], even though the present study used mixtures of PC and PG lipids. Other researchers studying the structure of pure PG lipid bilayers found a comparable lipid headgroup thickness PG lipids [5, 6], so the one value is employed in the SANS data analysis here.

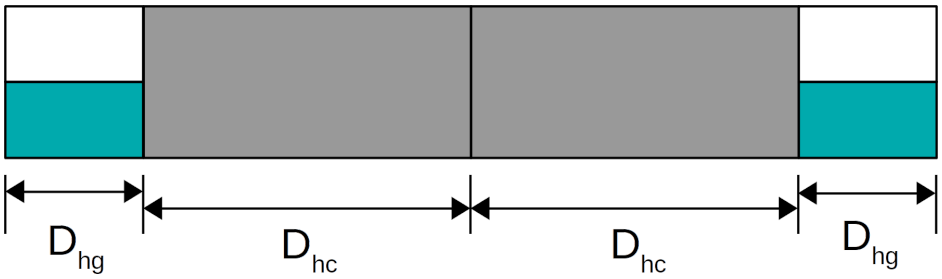

Figure S2: Schematic of the volumetric model of the lipid bilayer. The two hydrocarbon chain regions are shown in grey, the lipid headgroup is shown in teal and the water associated with the lipid headgroups are shown in white.

The composition of the lipid headgroup regions of the bilayer, which are assumed to be the same here, has to be determined in order to calculate the scattering length density (SLD), ρ, for use in the SANS intensity calculation. Much like the V_{hc} for a given sample, the average volume of the lipid

Group	b_{tot} (10^{-5} Å)	**Volume** (Å^3)	**Names**
PC Headgroup	60.09	320.0 [9]	$b_{PC,HG}$, $V_{PC,HG}$
PG Headgroup	91.776	300.0 [8]	$b_{PG,HG}$, $V_{PG,HG}$
Dimyristoyl chains	-29.06	780.0 [9]	b_{DM}, V_{DM}
Palmitoyl chain	-17.89	467.6 [10]	b_P, V_P
Oleyl chain	-12.09	468.4 [10]	b_O, V_O
gp41rk	842.08	2791.8 [11]	b_{gp41rk}, V_{gp41rk}
D_2O	19.14	30.0	b_{D_2O}, V_{D_2O}

Table S1: Parameters for SANS data analysis. Total neutron scattering lengths, b_{tot}, were calculated from the chemical composition and values of the atomic neutron scattering lengths provided by Sears [7]. The corresponding volumes of the chemical groups in the samples that were used to calculate the SLDs of the layers in the model were taken from literature values [8, 9, 10, 11]. Chemical groups on the PG headgroup and on gp41rk with exchangeable hydrogen atoms have these atoms replaced with deuterium for the calculation because the solvent is D_2O. The names of the parameters used in Equations S1-S9 are also provided.

headgroup, V_{Lhg}, is calculated from the sample composition and the values presented in Table 1. In addition to the lipid headgroups in these two regions of the model, this region of the model contains water and may contain peptide at the prepared peptide-to-lipid ratio, P/L, if it is present in the sample. The volume of the headgroup region of the bilayer is related to V_{Lhg}, D_{hg} and A_L, which in turn can be related to the number of water molecules in the region, n_w and any peptide associated with the headgroup region of the bilayer, as is shown in Equation 3.

$$V_{hg} = A_L D_{hg} = (P/L)V_p + V_{Lhg} + n_w V_{D_2O}. \tag{3}$$

Here, V_{D_2O} is the volume of a water molecule and V_p is the volume of the peptide, which are provided in Table S1. Using Equation 3, it is possible to calculate n_w for use in the calculation of the scattering length density of the lipid headgroup layers in the model during SANS data analysis.

$$n_w = \frac{A_L D_{hg} - (P/L) f_{insert} V_p - V_{Lhg}}{V_{D_2O}}. \tag{4}$$

The model requires only one other parameter, the fraction of peptide inserted across the bialyer, f_{insert}, to calculate the scattering length densities of the layers in the model. Additional parameters required for the modeling are the scale factor for the calculated SANS intensity profile and the constant baseline. In total, the structure used to model the SANS intensity profiles is parameterized using four free parameters (A_L, f_{insert}, the scale and the

baseline). The P/L and the fraction of DM lipids, f_{DM}, are also required for the model, but the are determined by the composition. The SLDs of the three layers in the model (the inner headgroup, hydrocarbon core and outer headgroup) are calculated using Equations 5 to 13.

$$b_{HG,in} = 0.7\, b_{PC,HG} + 0.3\, b_{PG,HG} + 0.5\, (1 - f_{insert})\, (P/L)\, b_{gp41rk} + n_w\, b_{D_2O}. \quad (5)$$

$$V_{HG,in} = 0.7\, V_{PC,HG} + 0.3\, V_{PG,HG} + 0.5\, (1 - f_{insert})\, (P/L)\, V_{gp41rk} + n_w\, V_{D_2O}. \quad (6)$$

$$\rho_{HG,in} = \frac{b_{HG,in}}{V_{HG,out}}. \quad (7)$$

$$b_{HC} = f_{DM}\, b_{DM} + (1 - f_{DM})\, (b_O + b_P) + 0.5\, f_{insert}\, (P/L)\, b_{gp41rk}. \quad (8)$$

$$V_{HC} = f_{DM}\, V_{DM} + (1 - f_{DM})\, (V_O + V_P) + 0.5\, f_{insert}\, (P/L)\, V_{gp41rk}. \quad (9)$$

$$\rho_{HC} = \frac{b_{HC}}{V_{HC}}. \quad (10)$$

$$b_{HG,out} = b_{HG,in}. \quad (11)$$

$$V_{HG,out} = V_{HG,in}. \quad (12)$$

$$\rho_{HG,out} = \frac{b_{HG,out}}{V_{HG,out}}. \quad (13)$$

3. SANS Data Analysis Results

Sample	χ^2 **range**	**scale**	**baseline**	A_L (Å^2)	f_{insert}
Lipid-1, P/L = 0	41.1843-41.1846	30.1 ± 0.1	0.0851 ± 0.0001	59.2 ± 0.1	0
Lipid-1, P/L = 1/50	36.8395-36.8502	32.2 ± 0.1	0.0827 ± 0.0001	59.7 ± 0.1	0.479 ± 0.236
Lipid-2, P/L = 0	42.9936-42.9937	29.6 ± 0.1	0.0822 ± 0.0001	65.1 ± 0.1	0
Lipid-2, P/L = 1/50	42.3150-42.3184	34.0 ± 0.1	0.0832 ± 0.0001	66.8 ± 0.1	0.345 ± 0.190
Lipid-3, P/L = 0	47.7750-47.7750	29.4 ± 0.1	0.0803 ± 0.0001	62.9 ± 0.1	0
Lipid-3, P/L = 1/50	35.9740-35.9757	34.9 ± 0.1	0.0813 ± 0.0001	63.7 ± 0.1	0.449 ± 0.273

Table S2: Results of the SANS data analysis. The values presented are the averages ± standard deviations, which were rounded up to the same number of significant figures as the values, that were found during the modeling as described in Section 2.5.

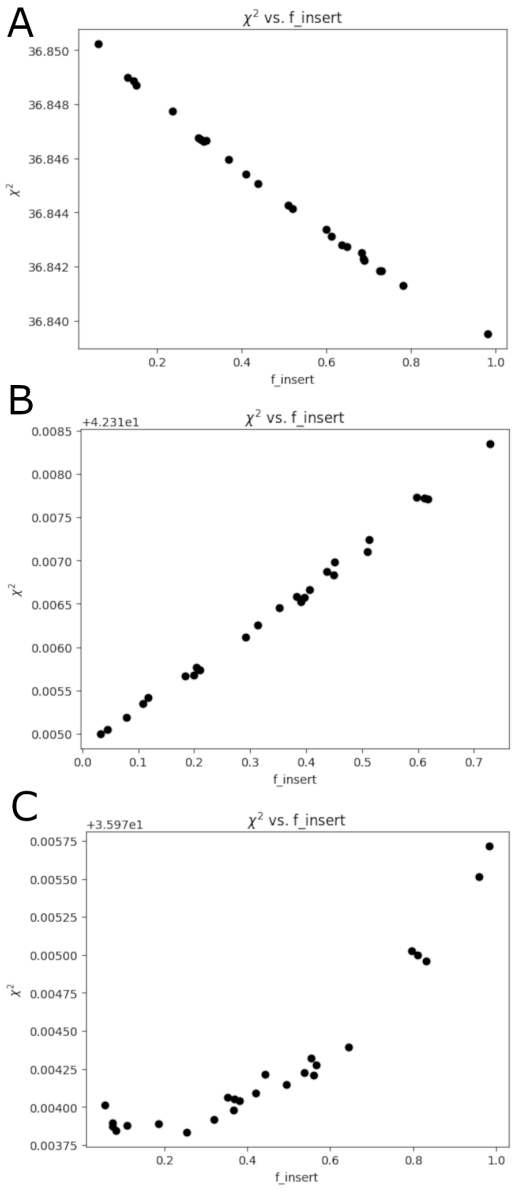

Figure S3: χ^2 vs. f_{insert} plots output by *sas-temper* [12] for Lipid-1 (A), Lipid-2 (B) and Lipid-3 (C) with gp41rk at P/L = 1/50.

4. NSE Data

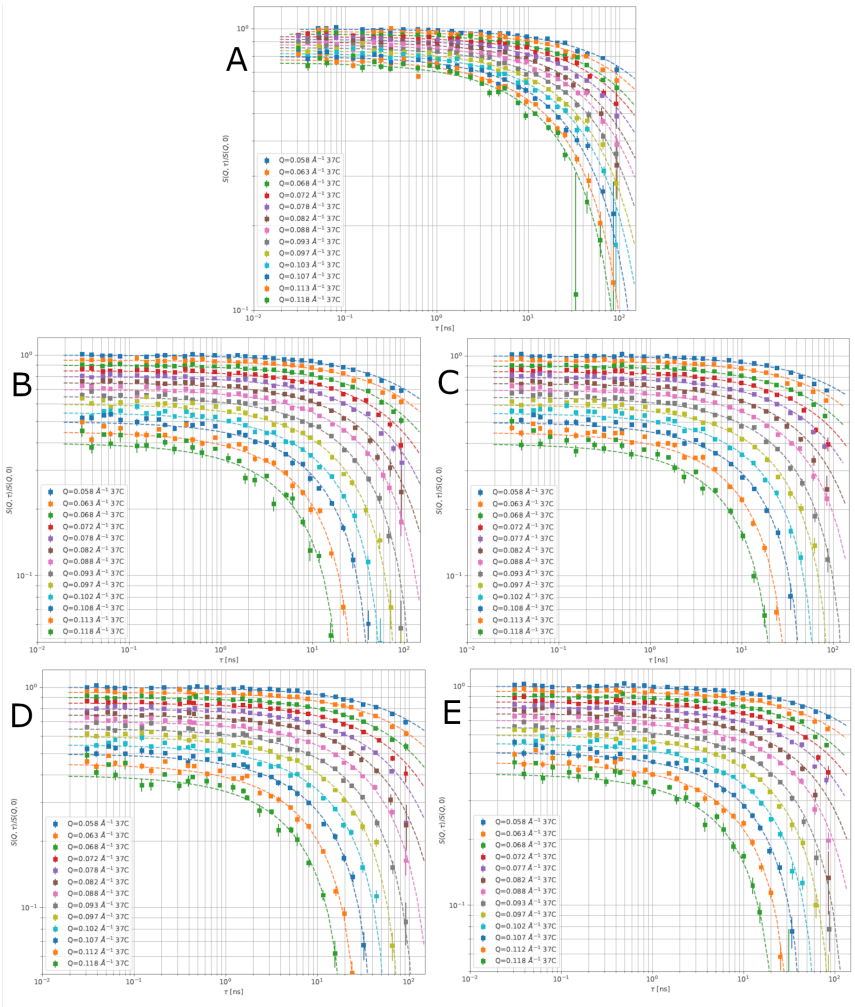

Figure S4: NSE data collected for the vesicles with and without gp41rk. Lipid-1 P/L = 1/50 (A), Lipid-2 P/L = 0 (B), Lipid-2 P/L = 1/50 (C), Lipid-3 P/L = 0 (D) and Lipid-3 P/L = 1/50 (E). The various q-values are shown in the figure legends. The symbols are the measured data points, while the lines are the fit to the data using Equation 1. The curves have been offset for clarity.

5. MD Simulations

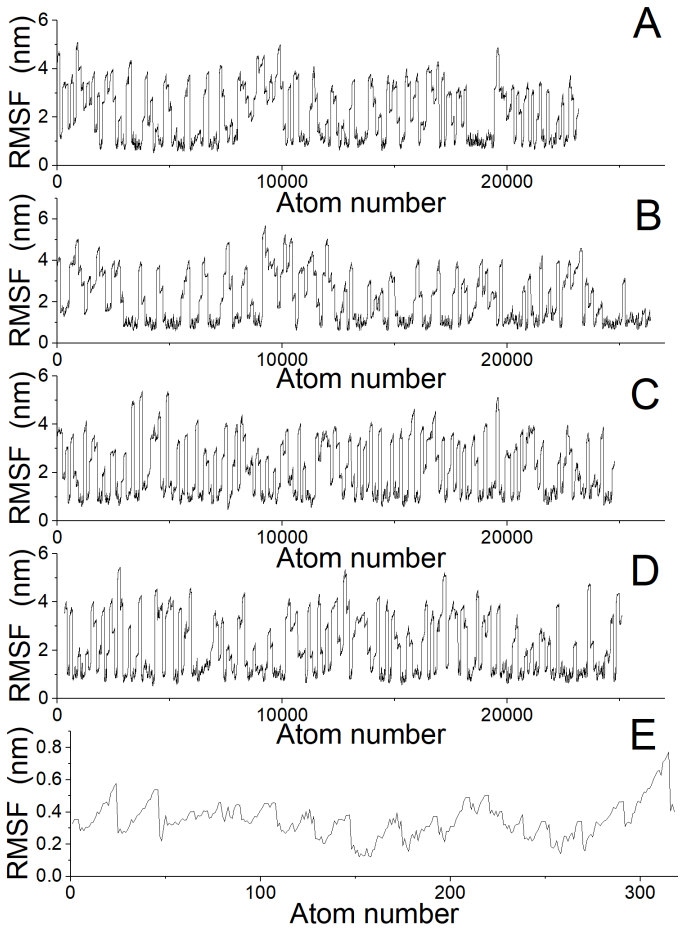

Figure S5: RMSF data for the lipids in the four simulations performed and the gp41rk from the Lipid-3/gp41rk simulation. Panel A is from the Lipid-1 simulation. The curve from Panel B is from the Lipid-2 simulation. Panel C is from the Lipid-3 simulation. Panel D is the lipid from the Lipid-3/gp41rk simulation, while Panel E is the peptide from that simulation.

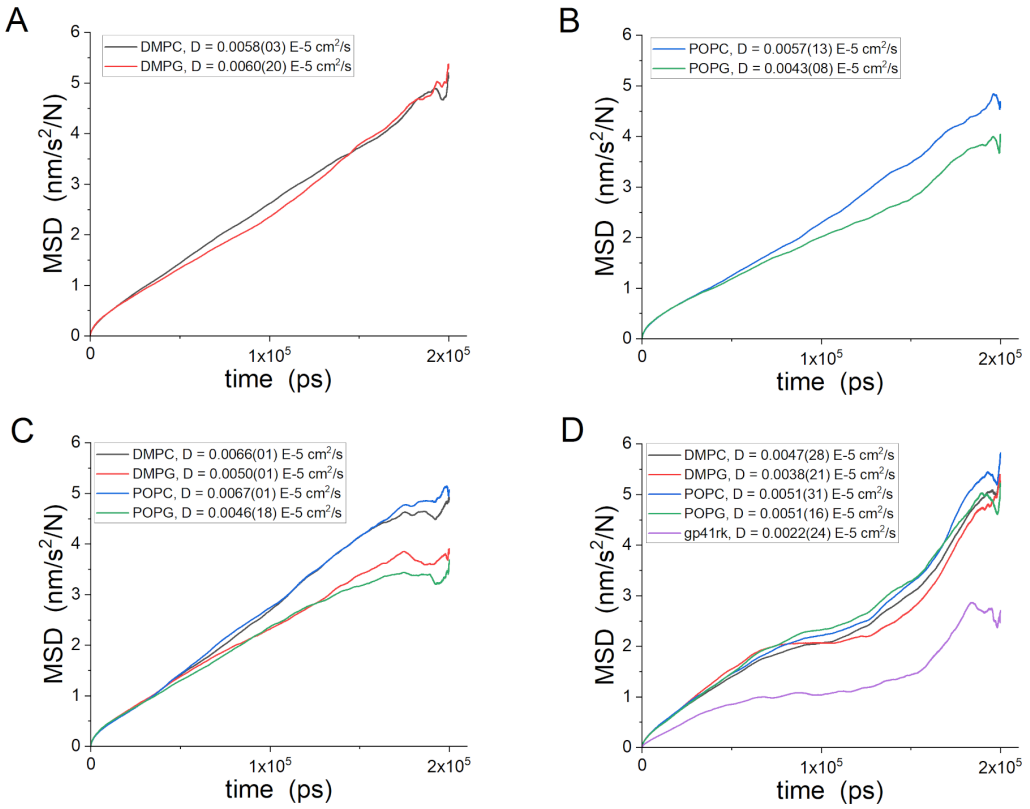

Figure S6: MSD and diffusion coefficients calculated from the four simulations performed. Panel A is from the Lipid-1 simulation, while Panel B is from the Lipid-2 simulation. The results from Lipid-3 are presented in Panel C, while the Lipid-3/gp41rk results are presented in Panel D. Diffusion coefficients determined using the default fitting parameters are shown in the legends of the figures.

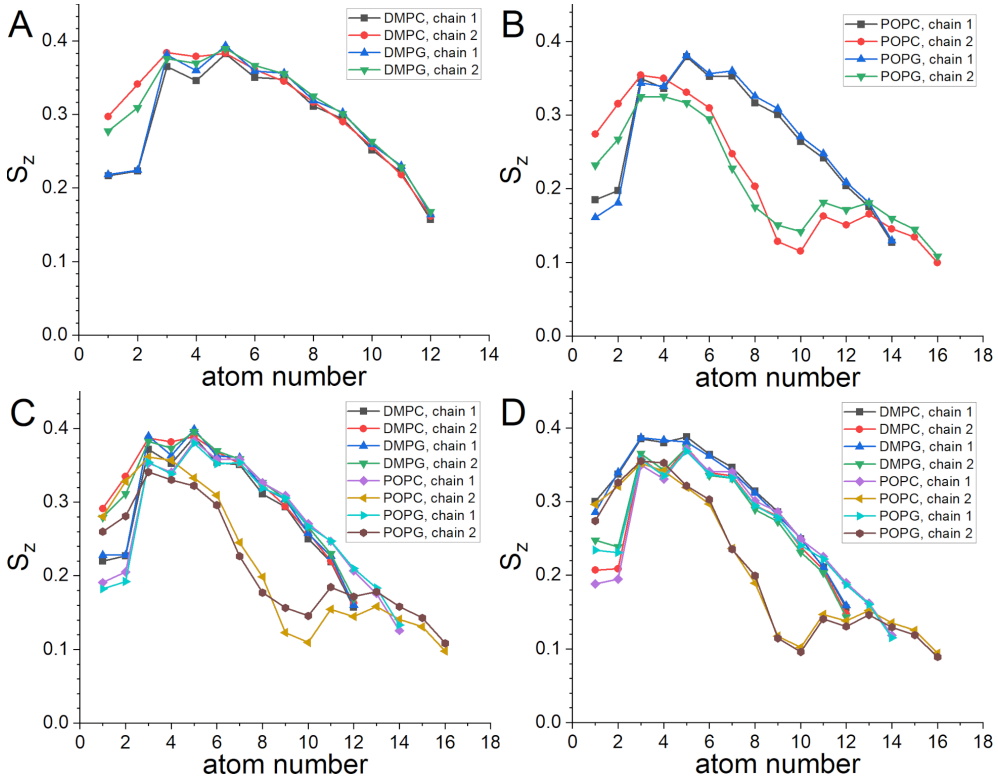

Figure S7: Chain order parameters from the MD simulations. Panel A is from the Lipid-1 simulation, Panel B shows the results from the Lipid-2 simulation, the order parameters from the Lipd-3 simulations are shown in Panel C, and the lipid order parameters calculated from the Lipid-3/gp41rk simulation are shown in Panel D.

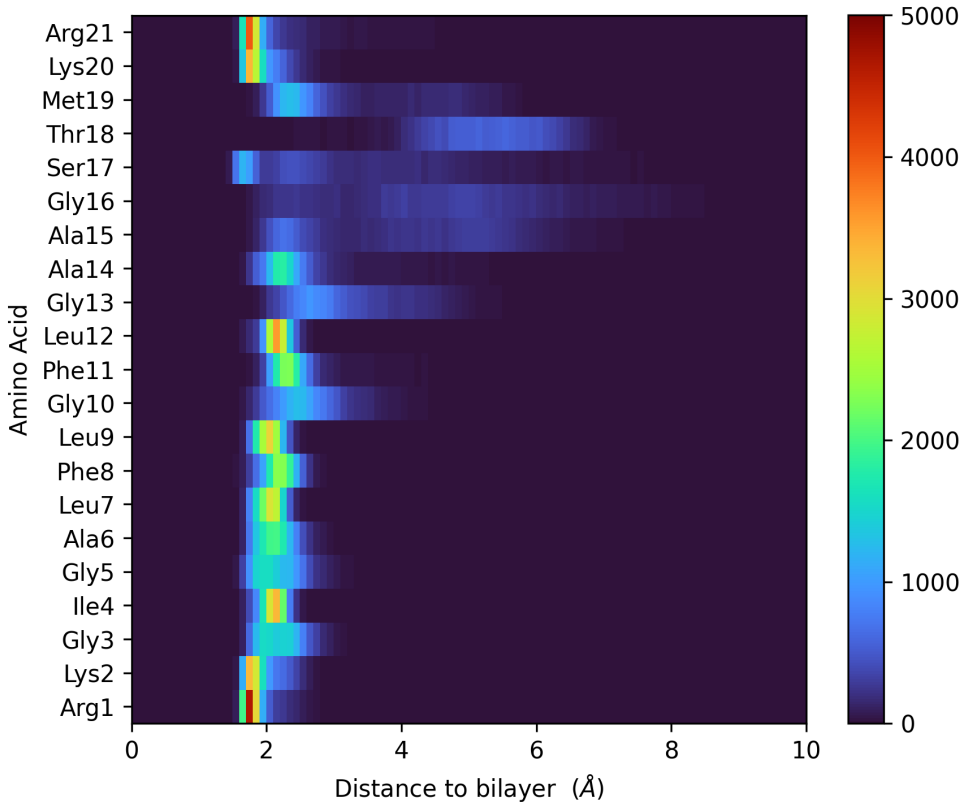

Figure S8: Histograms of the minimum distance between any lipid atom and the atoms of each amino acid residue of gp41rk. The calculated distances determined as a function of time during the Lipid-3/gp41rk simulation were used to create the histograms. The figure was generated from the output of *mindist* [13]. Custom Python code using Matplotlib [14] was written to create the figure from the output of *mindist*.

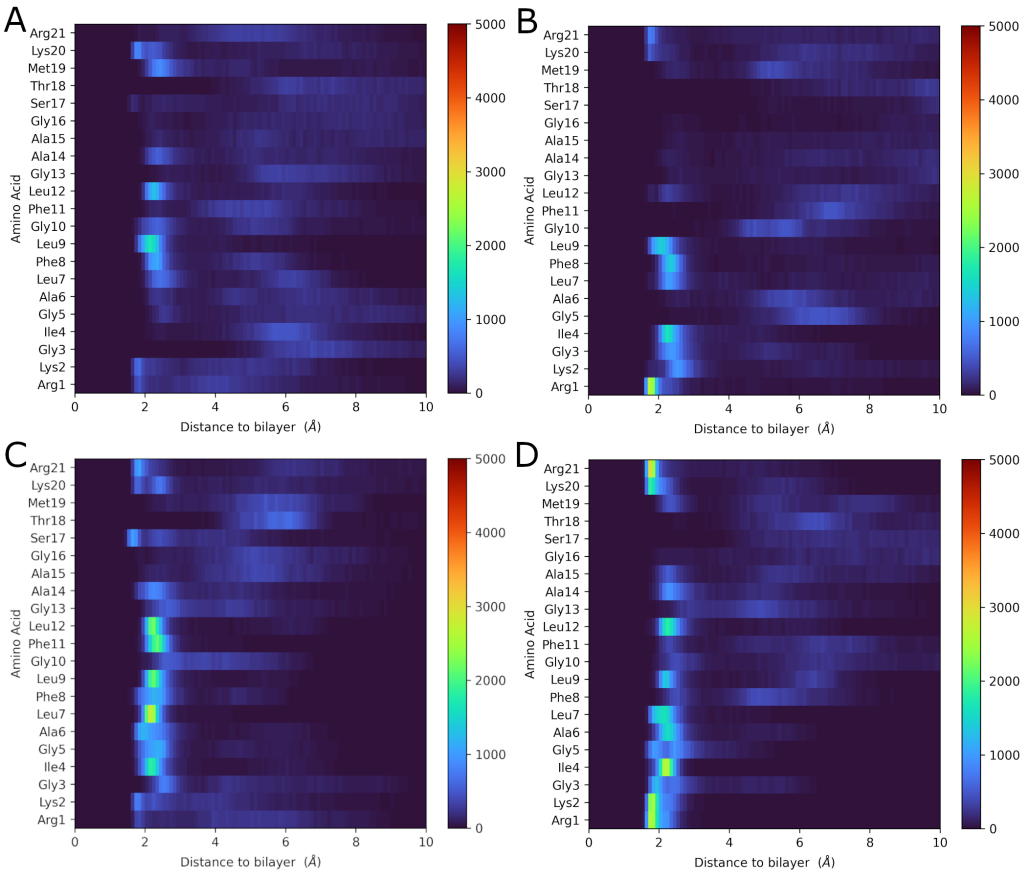

Figure S9: Histograms of the minimum distance between each type of lipid atom and the atoms of each amino acid residue of gp41rk. Panel A is DMPC, Panel B is DMPG, Panel C is POPC and Panel D is POPG. The calculated distances determined as a function of time during the Lipid-3/gp41rk simulation were used to create the histograms. The figure was generated from the output of *mindist* [13]. Custom Python code using Matplotlib [14] was written to create the figure from the output of *mindist*.

Funding

This research used resources at the Spallation Neutron Source, a DOE Office of Science User Facility operated by the Oak Ridge National Laboratory.

Acknowledgements

The authors would like to thank H. M. O'Neill and K. Weiss for access to the CD instrument, K. L. Weiss for access to the Bio-Labs at the Spallation Neutron Source and C. Gao and M. Odom for technical assistance during the neutron scattering experiments.

Conflict of Interest

The authors declare no conflict of interest.

References

[1] W. T. Heller, D. K. Rai, Changes in lipid bilayer structure caused by the helix-to-sheet transition of an hiv-1 gp41 fusion peptide derivative, Chemistry and Physics of Lipids 203 (2017) 46–53. doi:10.1016/j.chemphyslip.2017.01.004.

[2] W. T. Heller, P. A. Zolnierczuk, The helix-to-sheet transition of an hiv-1 fusion peptide derivative changes the mechanical properties of lipid bilayer membranes, Biochimica Et Biophysica Acta-Biomembranes 1861 (3) (2019) 565–572. doi:10.1016/j.bbamem.2018.12.004.

[3] W. T. Heller, A small-angle neutron scattering study of the physical mechanism that drives the action of a viral fusion peptide, Chemistry and Physics of Lipids 234 (JAN 2021). doi:10.1016/j.chemphyslip.2020.105022.

[4] J. F. Nagle, S. Tristram-Nagle, Structure of lipid bilayers, Biochimica et Biophysica Acta (BBA) - Reviews on Biomembranes 1469 (3) (2000) 159–195. doi:10.1016/S0304-4157(00)00016-2.

[5] N. Kučerka, B. W. Holland, C. G. Gray, B. Tomberli, J. Katsaras, Scattering density profile model of popg bilayers as determined by molecular dynamics simulations and small-angle neutron and x-ray scattering experiments, The Journal of Physical Chemistry B 116 (1) (2012) 232–239. doi:10.1021/jp208920h.

[6] J. Pan, F. A. Heberle, S. Tristram-Nagle, M. Szymanski, M. Koepfinger, J. Katsaras, N. Kučerka, Molecular structures of fluid phase phosphatidylglycerol bilayers as determined by small angle neutron and x-ray scattering, Biochimica et Biophysica Acta (BBA) - Biomembranes 1818 (9) (2012) 2135–2148. doi:10.1016/j.bbamem.2012.05.007.

[7] V. F. Sears, Neutron scattering lengths and cross sections, Neutron News 3 (3) (1992) 26–37. doi:10.1080/10448639208218770.

[8] J. Marra, Direct measurement of the interaction between phosphatidylglycerol bilayers in aqueous electrolyte solutions, Biophysical Journal 50 (5) (1986) 815–825. doi:10.1016/S0006-3495(86)83522-6.

[9] R. S. Armen, O. D. Uitto, S. E. Feller, Phospholipid component volumes: Determination and application to bilayer structure calculations, Biophysical Journal 75 (2) (1998) 734–744. doi:10.1016/S0006-3495(98)77563-0.

[10] N. Kučerka, S. Tristram-Nagle, J. F. Nagle, Structure of fully hydrated fluid phase lipid bilayers with monounsaturated chains, Journal of Membrane Biology 208 (3) (2005) 193–202. doi:10.1007/s00232-005-7006-8.

[11] B. Jacrot, The study of biological structures by neutron scattering from solution, Reports on Progress in Physics 39 (10) (1976) 911–953. doi:10.1088/0034-4885/39/10/001.

[12] W. T. Heller, M. Doucet, R. K. Archibald, Sas-temper: Software for fitting small-angle scattering data that provides automated reproducibility characterization, SoftwareX 16 (2021) 100849. doi:10.1016/j.softx.2021.100849.

[13] M. J. Abraham, T. Murtola, R. Schulz, P. S., J. C. Smith, B. Hess, E. Lindahl, Gromacs: High performance molecular simulations through multi-level parallelism from laptops to supercomputers, SoftwareX 1-2 (2015) 19–25. doi:10.1016/j.softx.2015.06.001.

[14] J. D. Hunter, Matplotlib: A 2d graphics environment, Computing in Science & Engineering 9 (3) (2007) 90–95. doi:10.1109/MCSE.2007.55.